Research Article

Ye Yang, Yawovi Souley Agbodjan, and Bo Liang*

Study of fracturing fluid re-discharge based on percolation experiments and sampling tests – An example of Fuling shale gas Jiangdong block, China

https://doi.org/10.1515/geo-2022-0537
received July 04, 2023; accepted August 30, 2023

Abstract: Shale gas development requires the use of hydraulic fracturing, and the relationship between fracturing fluid drainage and production is not clear. Therefore, it is necessary to adopt the method of core experiment combined with engineering validation to achieve the description of the seepage-absorption-return mechanism of shale and to optimize the selection of fracturing fluids and the testing work system in engineering. In this study, a "seepage experiment → sampling test → engineering validation" working procedure is proposed, and it is found that seepage occurs only on the surface of the fracture where the liquid medium intrudes into the fracture and that the amount of water absorbed is directly proportional to the area of seepage; the rate of return is inversely proportional to the production rate in the same secondary tectonic unit; and the absorption rate per unit area of four types of cores with the same surface area is directly proportional to the yield of the fractured shale in the same medium. Under the premise of the same medium, the water absorption per unit area of the four types of cores varies with the rate of change with time, but the general trend is the same. Under the premise of different secondary tectonic units, when the time of good closure is similar, the correlation between the return rate and the test production is weak.

Keywords: shale gas, fracturing fluid, imbibition, backward discharge, sample survey

1 Introduction

Shale gas reserves are vast, but the dense nature of shale reservoirs necessitates hydraulic fracturing for commercial exploitation [1]. As a result, the industry primarily focuses on shale reservoir fracturing, hydration, imbibition, shut-in, and flowback. In engineering, the flowback rate of shale gas wells after fracturing is generally low, typically only reaching 35–62% within 1 year [2]. Shale formations contain significant amounts of clay minerals, which can lead to hydration. However, the impact of this process on shale gas productivity remains unknown [3]. Additionally, different fracturing fluid systems with varying compositions and water content can affect the final production. Hence, it is crucial to study the mechanism of fracturing fluid backflow.

In terms of theoretical guidance, current research focuses on improving the accuracy of existing scientific problems through mathematical models, physical models, and conducting engineering observations or experimental research in unknown areas. For example, Qu et al. [4] developed a more accurate comprehensive flowback model for fracturing fluid by modifying the calculation model for proppant settling velocity, introducing a new calculation model for critical proppant backflow velocity, and incorporating a wellhead pressure calculation model. The average errors of this model were found to be 11.9 and 11.6%, respectively. In terms of engineering, it has been concluded that selecting smaller fracturing fluid density and proppant particle sizes can lead to greater flowback efficiency and reduced proppant settling. Chen and Wang [5] established a mathematical model for shale water–rock interaction during fracturing fluid backflow. This new model considers multiphase flow in fractured shale reservoirs and forms a comprehensive numerical simulator. The results quantify the effects of chemical infiltration, clay swelling, and mineral dissolution. Liu et al. [6] proposed a particle tracking method

* **Corresponding author: Bo Liang**, School of Aviation and Transportation, Jiangsu College of Engineering and Technology, Nantong 226000, China, e-mail: bliang0325@163.com
Ye Yang, Yawovi Souley Agbodjan: School of Energy Science and Engineering, Central South University, Changsha 410083, China

to study the phenomenon of proppant backflow in meso-scale hydraulic fracturing fractures during the flowback of fracturing fluid. The flowback process of fracturing fluid was simulated using the steady Navier–Stokes equation. Wang et al. [7] developed a comprehensive mixed model to analyze the characteristics of two-phase flow and predict production performance in tight gas wells with three-dimensional discrete fractures. The transient flow equation in this model was solved numerically using the finite difference method, and the flow behavior in the reservoir was determined using three-dimensional volume source functions and the superposition principle. Elputranto et al. [8] used a fully coupled non-isothermal multi-component two-phase flow equation with geomechanics to simulate formation damage caused by hydraulic fracturing in shale gas wells. It was discovered that the mechanism of formation damage is mainly a multi-physical/chemical problem that develops near the interface between the fracture and the matrix.

In terms of methodological orientation, current research efforts primarily focus on proposing targeted solutions to scientific problems from a theoretical standpoint. These solutions then lead to the development of optimization schemes, experimental configurations, and analytical models. For instance, Hun et al. [9] conducted self-priming and reverse flooding experiments on shale formations and utilized low-field nuclear magnetic resonance technology to monitor the volume change of liquid in shale core samples. They calculated the volume change of liquid in the pores at different time intervals. Shidhani et al. [10] compared the production effects of two scenarios: direct flowback after hydraulic fracturing and flowback after a long-term shut-in period. The study concluded that appropriate drainage and production systems can effectively reduce reservoir damage and limit the production impact caused by the difference in drainage and production conditions. Saini et al. [11] developed a flowback additive based on nano-emulsion specifically designed for oil-bearing sandstone and carbonate formations. These flowback additives exhibited low surface tension (22–30 mN/m) and interfacial tension (<6 mN/m). When the nano-emulsion particle size ranged from 5 to 15 nm, these additives were able to prevent emulsion formation with crude oil and effectively reduce capillary pressure, thereby enhancing productivity. Osselin et al. [12] employed the isotope tracer method to quantify the extent of fracturing fluid flowback. They discovered that only one-third of the water used in hydraulic fracturing with a nitrogen-water mixture was able to be recovered from the Montney formation in Alberta. Owen et al. [13] used chloride concentration, oxygen, and hydrogen isotopes as tracers to calculate the proportion of returned water from 24 specifically completed wells in a research area. The study concluded that a significant portion of the fracturing fluid remains in the reservoir due to imbibition, and there is also a substantial volume of original formation water present.

In terms of result orientation, current research focuses on obtaining qualitative and quantitative conclusions regarding engineering problems through experimental and engineering methods. Researchers propose engineering hypotheses and aim to validate them. For instance, Wu et al. [14] utilized nuclear magnetic resonance and fracture visualization models to qualitatively and quantitatively describe the impact of connectivity between primary and secondary fractures on flowback. Yang et al. [15] conducted experiments to quantitatively evaluate the water absorption capacity of shale in the Sichuan Basin, China. They found that water absorption in shale primarily occurs along shale bedding and micro-cracks. The arrangement of minerals enhances adsorption, and shale with a micro-fracture network exhibits a high adsorption rate. Verdugo and Doster [16] analyzed the influence of capillary pressure and flowback operations on productivity using numerical reservoir simulation. The study concluded that, with low capillary pressure, shortening the shut-in time leads to better productivity. Conversely, in cases with high capillary pressures, longer shut-in times result in improved productivity. Wang et al. [17] visualized and quantitatively characterized the dynamic flowback process of different fracturing fluids in the Songliao Basin using nuclear magnetic resonance technology. The compatibility between fracturing fluid and shale oil reservoirs was also discussed. Chen et al. [18] discussed the treatment and recovery technology of acid fracturing fluid and observed that calcium and magnesium ions can affect the crosslinking performance of acid fracturing fluid.

Research conducted under different orientations is crucial for understanding the mechanism of fracturing fluid flowback. This is particularly important in exploratory well areas where regional geological characteristics are not well defined. In such cases, fracturing tests often rely on theoretical-oriented mathematical models and calculation formulas to guide fieldwork. Currently, theoretical research has demonstrated that imbibition is a phenomenon where the non-wetting phase is replaced by the wetting phase under capillary pressure [19]. Understanding the characteristic patterns of this phenomenon is highly significant for the exploitation of oil and gas resources in tight reservoir matrices. Compared to previous studies, the present study focuses more on combining core experiments with engineering verification. Many researchers typically rely on simulation software for macroscopic analyses, but these conclusions can be inaccurate [20]. In this study, a new approach of "geological study → experiment → engineering validation" is proposed for the Fuling shale

gas Jiangdong block in China. This study is valuable for enhancing the selection and testing system of fracturing fluids in the field. The research problem in this study can be summarized as follows: (1) The aim of the study is to understand the phenomenon of shale water absorption and the impact of imbibition area on shale imbibition through dynamic imbibition experiments. (2) The study investigates the water absorption per unit area of shale in various liquid media and examines the factors influencing it through static imbibition experiments. (3) By conducting sampling inspections, the study compares the flowback data obtained after different shut-in times, considering different secondary structural units, as well as the flowback data obtained after the same shut-in time, considering the same secondary structural unit. (4) The study also includes an engineering verification to determine if the experimental results align with the actual engineering practices.

2 Research background

The productivity of shale gas in a single well is primarily influenced by its structural characteristics. These structural elements can be further classified into structural burial depth, structural morphology, and fracture development characteristics [21]. First-order faults that control the structural boundary and second-order faults that control the structural belt have a significant impact on the preservation conditions of shale gas. However, third- and fourth-order faults that control local structure or adjust the structure have minimal influence on shale gas preservation conditions. Due to these fault divisions, the physical properties of different secondary structural units within the reservoir vary. This study focuses on the Jiangdong block of Fuling shale gas and specifically examines the production test link within its research boundary [20]. The objective of this research is to investigate the mechanism of fracturing fluid flowback through core experiments. The preset coring wells are used to maintain consistency in the scale of fracturing, while solely considering the influence of structural characteristics on shale gas productivity.

The study area is located in Fuling District, Chongqing, specifically in the Jiangdong block. This block is situated in the southeastern region of the Wanxian syncline, which is a high-steep structural belt in eastern Sichuan. It is positioned at the convergence point of the Jiaoshiba anticline belt, Wujiang anticline belt, and Tiantaichang syncline belt. As it transitions from the Jiaoshiba block to the Tiantaichang syncline, the burial depth of the strata progressively deepens, forming a downward-dipping monoclinic structure [22]. The Jiangdong block can be divided into two structural belts, namely, the northern and southern belts, each consisting of multiple secondary structural units. The northern belt, which exhibits a more complex structural form compared to the Jiaoshiba block, can be subdivided into four secondary structural units. These include the west wing of the Jiaoshiba fault anticline (North Area 1), Tiantaichang No. 2 fault nose (North Area 2), Diaoshuiyan syncline (North Area 3), and Tiantaichang No.1 fault nose (North Area 4). These units are distributed in a northeast direction. On the other hand, the southern belt can be subdivided into two sub-structural units, namely, Jiangdong Anbu (South Area 1) and Wujiang No. 1 fault anticline (South Area 2). These units are distributed in the northwest direction [23,24]. The study area exhibits two groups of faults with different strike directions. The faults near the Wujiang fault zone in the southwest are primarily oriented in a north-south direction. In contrast, most other faults in the region exhibit a northeast-striking trend [25]. As one moves from north to south within the study area, the degree of structural deformation and fault development gradually becomes more intricate (Figure 1).

The Jiangdong block is characterized by well-developed faults, with a total of 48 reverse faults identified. These faults predominantly strike in the northeast direction. Among these faults, there are three boundary faults that exhibit a fault distance greater than 100 m. These boundary faults play a significant role in controlling local structures within the study area. Additionally, there are 28 faults with a fault distance ranging from 50 to 100 m, most

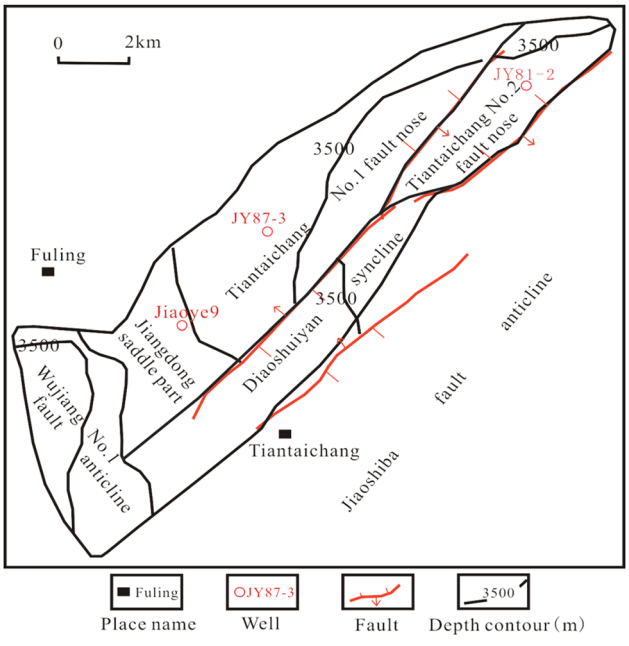

Figure 1: Structural map of Jiangdong block of Fuling shale gas.

of which are adjacent to larger faults. Furthermore, 17 faults have a fault distance of less than 50 m, primarily associated with faults that have a fault distance of 50–100 m. The faults within the central part of the entire structure show limited development.

The reservoir in the Jiangdong block consists of the Upper Ordovician Wufeng Formation and Lower Silurian Longmaxi Formation. These formations represent a deep-water shelf depositional environment. The reservoir can be divided into nine sub-layers, starting from the bottom to

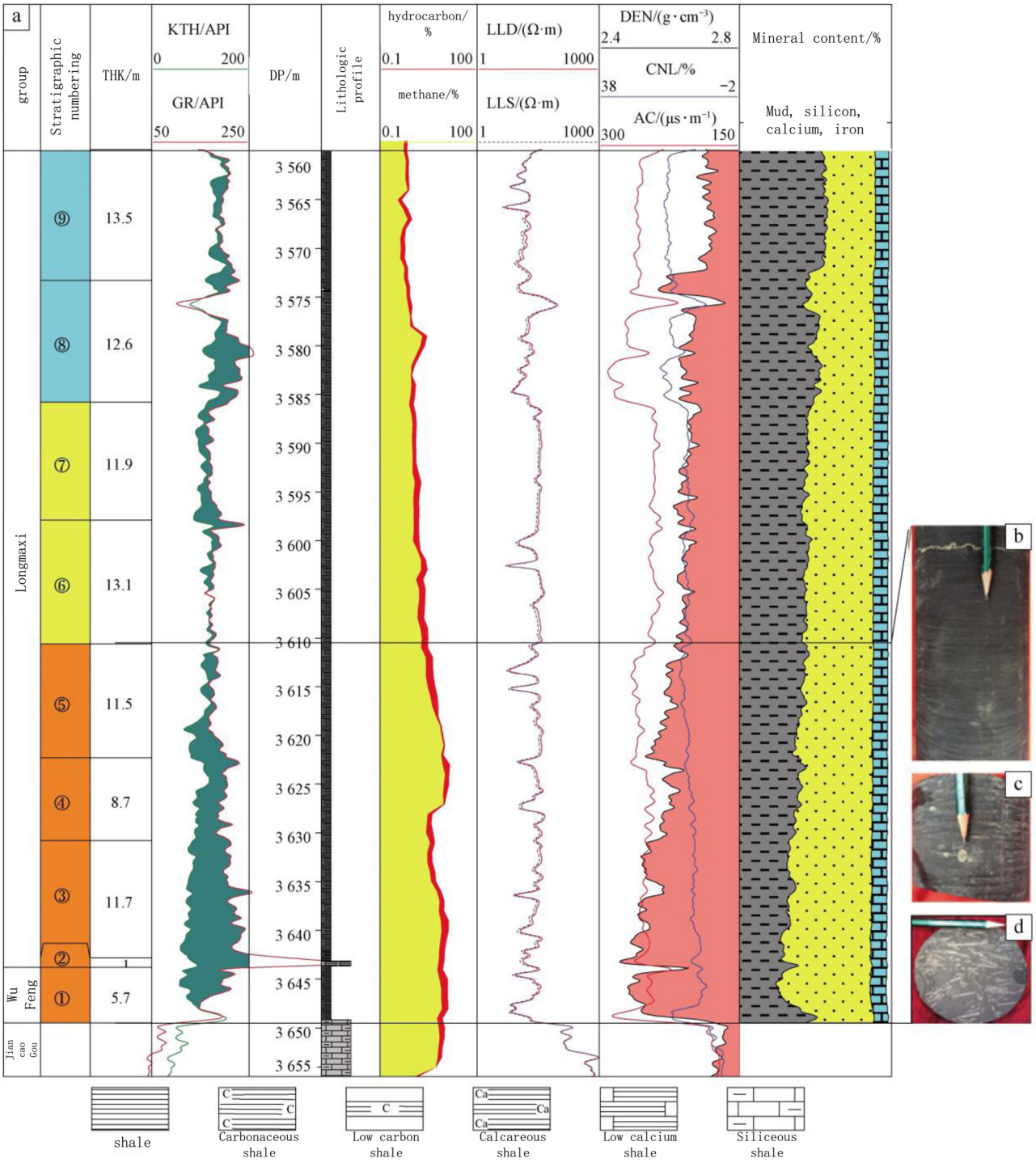

Figure 2: Three-end meta-plot of rock minerals in the Upper Ordovician Wufeng Formation and Lower Silurian Longmaxi Formation of the Jiangdong block.

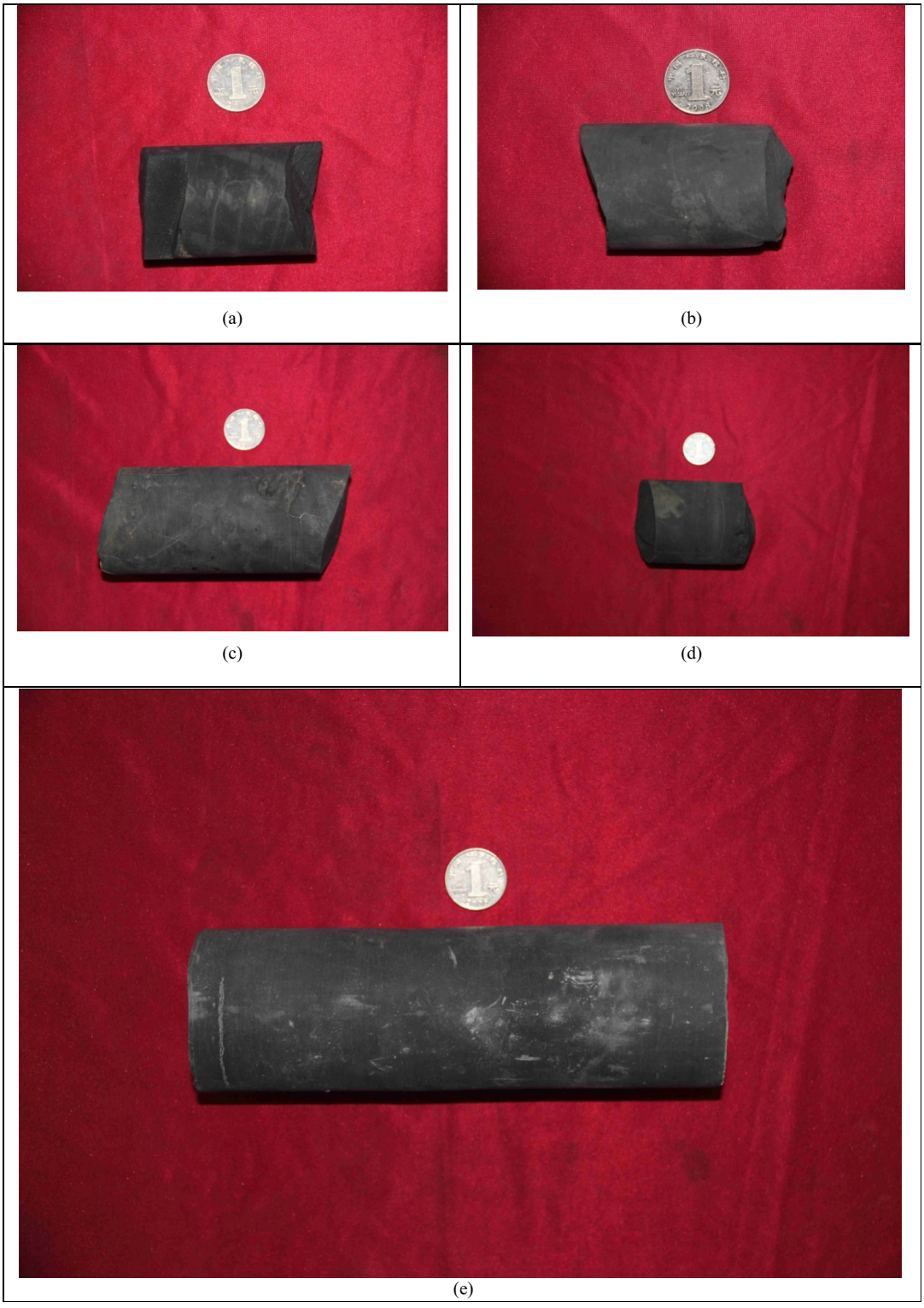

Figure 3: Core sample diagram. (a) Black silty shale with microscopic bedding and massive structure. (b) Black siliceous shale with massive structure. (c) Black mud shale, see horizontal bedding, with developed cracks and filled with calcite. (d) Black mud shale, with developed cracks and filled with calcite, with massive structure. (e) Black shale, slightly bedded on the side, massive structure, calcite vein.

the top. The average content of brittle minerals in the reservoir is 59.35%, while clay minerals make up the remaining 40.65%. In terms of organic matter abundance, the average total organic carbon (TOC) content in the sub-layers (1)–(5) ranges from 3.10 to 3.48%. For the sub-layers (6)–(9), the average TOC content is slightly lower, ranging from 2.69 to 2.90%. The average porosity of the reservoir is 4.74%. Interestingly, the correlation between gas saturation and burial depth is minimal. At a depth of 3,500 m, the gas saturation is approximately 65%. However, production data from 39 wells indicate that the production in areas with burial depths greater than 3,500 m is low. In fact, test production from individual wells shows a negative correlation with burial depth, as illustrated in Figure 2.

To summarize, the Jiangdong block is characterized by both south and north structural belts, along with five secondary structural units. To gather more information about these units, core samples were collected from representative wells in each unit, and basic data were measured. These measurements are crucial in preparing for future experiments and analysis. Please refer to Figure 3 and Table 1 for the specific details of the measured data.

This study follows a five-step process. First, the research scope is established by focusing on the Fuling shale gas in the Jiangdong block. Basic geological research is conducted, and representative well cores are collected to determine basic physical parameters. In the second step, static imbibition experiments are set up, and the water absorption per unit area of the five cores is measured after contacting them with four different media. The third step involves setting up a dynamic imbibition experiment and measuring the overall water absorption data of the five cores under the four different media conditions. In the fourth step, a sampling comparison scheme is formed using the sampling inspection method. This scheme includes comparing shut-in time flowback data from different secondary structural units and comparing shut-in time flowback data from the same secondary structural unit under different conditions. Finally, in the fifth step, all previous research results are integrated. The sampling inspection scheme is implemented to verify the actual experimental conclusions of the project. The logical flow of the research process is presented in Figure 4.

The supplementary explanation of this study includes the following details: (1) Five cores were selected from five different secondary structural units to ensure that the study covers a wide range of physical properties of the reservoirs in the study area. The cores were taken in their original wet state to accurately represent the conditions of the reservoir. (2) The study utilizes four different media for the imbibition experiments: distilled water, formation water, fracturing fluid A, and fracturing fluid B. This selection allows for a comprehensive simulation of the underground environment and theoretical laboratory conditions. (3) A total of 67 wells in the study area have been completed and put into production. The sampling inspection scheme was applied to two different scenarios of the imbibition experiment, effectively achieving the goal of scientific demonstration. These additional details provide a clear understanding of the specific methods and conditions used in the study, enhancing its scientific validity.

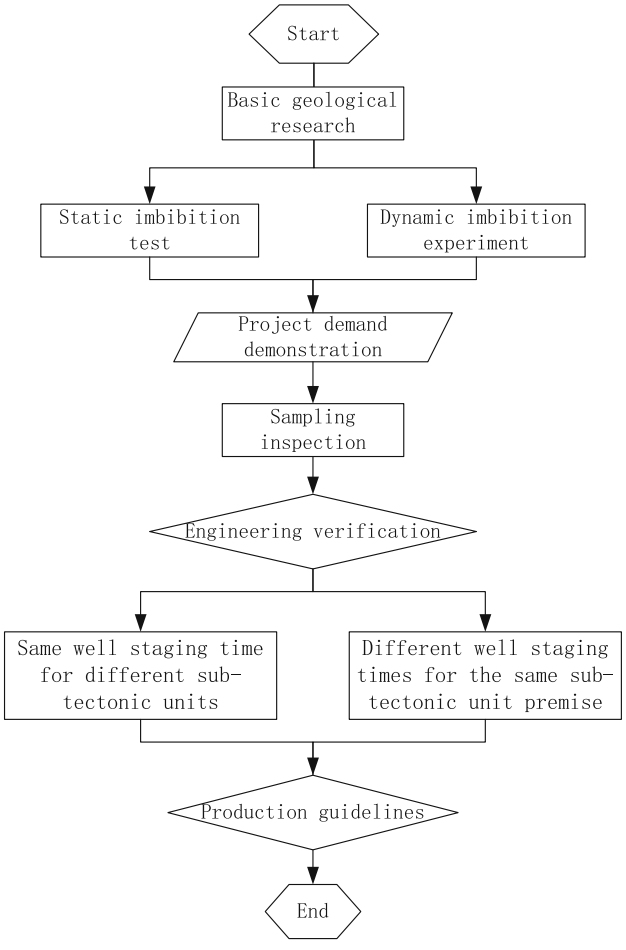

Figure 4: Logic diagram of research process.

Table 1: Geological data of sampled cores

Core number	Average TOC (%)	Brittle mineral content (%)	Clay mineral content (%)	Osmotic area (cm^2)
a	2.99	56.98	43.02	4.99
b	2.93	54.33	45.67	4.99
c	2.91	53.29	46.71	7.61
d	3.14	57.21	42.79	12.34
e	2.74	55.21	44.79	10.15

*Imbibition area = core face area + face rubbings crack area.

3 Experimental investigation

3.1 Materials and methods

3.1.1 Imbibition experiment

The study recognized that different fracturing fluid systems and fluid qualities can result in varied shale imbibition outcomes. Additionally, the flowback rate can also be affected by different shale samples due to variations in lithology and natural fracture development. To address these factors, experiments were conducted to explore the imbibition characteristics of five cores from five secondary structural units in the study area when exposed to distilled water, formation water, fracturing fluid A, and fracturing fluid B.

The experimental setup included the following materials and equipment: a METTLER electronic balance, an oven, a static water saturation measuring bench (Figure 5), a dynamic imbibition test bench (Figure 6), high purity methane, five cores (meeting specific preparation standards: length 4.81 cm, diameter 2.51 cm, and end face area 4.99 cm^2), distilled water (viscosity 0.890 MPa s), formation water (salinity 80,000 mg/L and viscosity 0.980 MPa s), fracturing fluid A (viscosity 1.832 MPa s), and fracturing fluid B (viscosity 3.771 MPa s). These experimental details were crucial in accurately assessing the effects of different fluids and shale characteristics on the imbibition process.

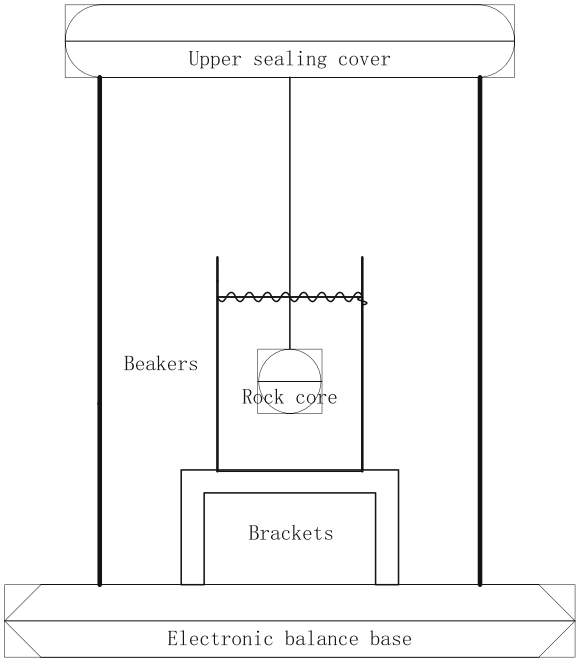

Figure 5: Diagram of static imbibition measuring device.

In the static imbibition experiment, the following steps were followed: (1) Begin by drying five cores in an oven at a temperature of 110°C for 24 h. After cooling, decompose each core into four spheres, resulting in a total surface area of 11.452 cm^2 based on the size of the beaker. (2) Next debug the test bench and add the experimental medium into the beaker. Make sure the test bench is functioning properly. (3) Hang the dried samples using thin wires and carefully place them into the medium swiftly. Ensure that the samples are immersed smoothly and quickly without any disturbances. (4) Seal the experimental container to maintain a controlled environment and start recording the continuously changing weight values of the samples. (5) Repeat the above steps for each of the five cores, measuring the data for each core when in contact with the four different media. It is important to record the increase in mass at each time point during the experiment for further analysis. Following these steps allows for the collection of accurate data to analyze the imbibition characteristics of the shale samples when exposed to different fluids.

In the dynamic imbibition experiment, the following steps were followed: (1) Begin by testing the airtightness of the test bench. Start the electronic components for 3 min and calibrate the simulation data. Ensure that the transmission and decoding of the PLC are functioning normally and that the calculation of the electronic indicator terminal is accurate. (2) Dry all cores in an oven at a temperature of 110°C for 24 h. After cooling, measure the weight of each core and place them in the core holder. (3) Set the thermostat to 80°C and introduce N_2 medium into the system. Use a confining pressure pump to pressurize the core holder to 20 MPa, simulating the formation pressure. (4) Open regulating valve 1 and use a power pump to inject the experimental medium into the core at a constant flow rate of 0.2 mL/min. Let the flow pattern stabilize and run the test bench continuously for 24 h. (5) After the 24-h operation, turn off the confining pressure pump and power pump. Open regulating valve 2 to discharge the experimental medium and open regulating valve 3 to release the pressurized N_2. Remove the core from the holder, observe the invasion of the medium, and measure the weight of the core. (6) Repeat the above steps for each of the five cores, measuring the data under four different media conditions. Calculate the water absorption based on the weight measurements and further analyze the dynamic imbibition characteristics of the shale samples. By following these steps, accurate data can be collected and analyzed to understand the dynamic imbibition behavior of the shale cores under different media conditions.

3.1.2 Sampling inspection

In order to validate the accuracy of the imbibition experiment results and enhance the practical implications for engineering applications, it is crucial to compare the fracturing flowback data of two different types of fracturing fluids – fracturing fluid A (comprised of integrated variable viscosity drag reduction water) and fracturing fluid B (carboxymethyl hydroxypropyl guar gum). Additionally, it is necessary to conduct a comparative analysis of flowback data obtained at the same shut-in time but with different secondary structural units, as well as flowback data obtained at different shut-in times while maintaining the same secondary structural unit. By performing this comparative analysis, it will be possible to assess the effectiveness of the two different fracturing fluids in terms of flowback characteristics. The influence of different secondary structural units and shut-in times on the flowback behavior can also be evaluated. This comparative analysis will provide valuable insights into selecting the most suitable fracturing fluid for specific reservoir conditions and optimizing the shut-in time for efficient flowback operations.

In this study, a total of 67 wells were completed and put into production in the Jiangdong block, which consists of 5 secondary structural units. However, due to variations in fracturing time, construction designs, bridge plug types, and fracturing fluids used, the shut-in time of the test wells under real working conditions is unpredictable and irregular. To overcome this challenge, a systematic approach needs to be followed to sample and analyze the flowback data. For the sampling of flowback data at the same shut-in time under the premise of different secondary structural units, it is important to identify wells with similar shut-in time while using the same fracturing fluid. This will ensure a fair comparison between the secondary structural units. Five representative wells from each of the five secondary structural units can be selected based on these criteria. On the other hand, for the sampling of flowback data at different shut-in times in the same secondary structural unit, it is suggested to sample data at commonly occurring shut-in times such as 0, 3, 5, 7, 9, 10, 15, 17, 20, 22, 25, and 30 days. However, this analysis should account for the variations in fracturing fluids, shut-in time, fracturing scale, and testing pressure among different wells. Taking these factors into consideration, it is important to carefully organize and

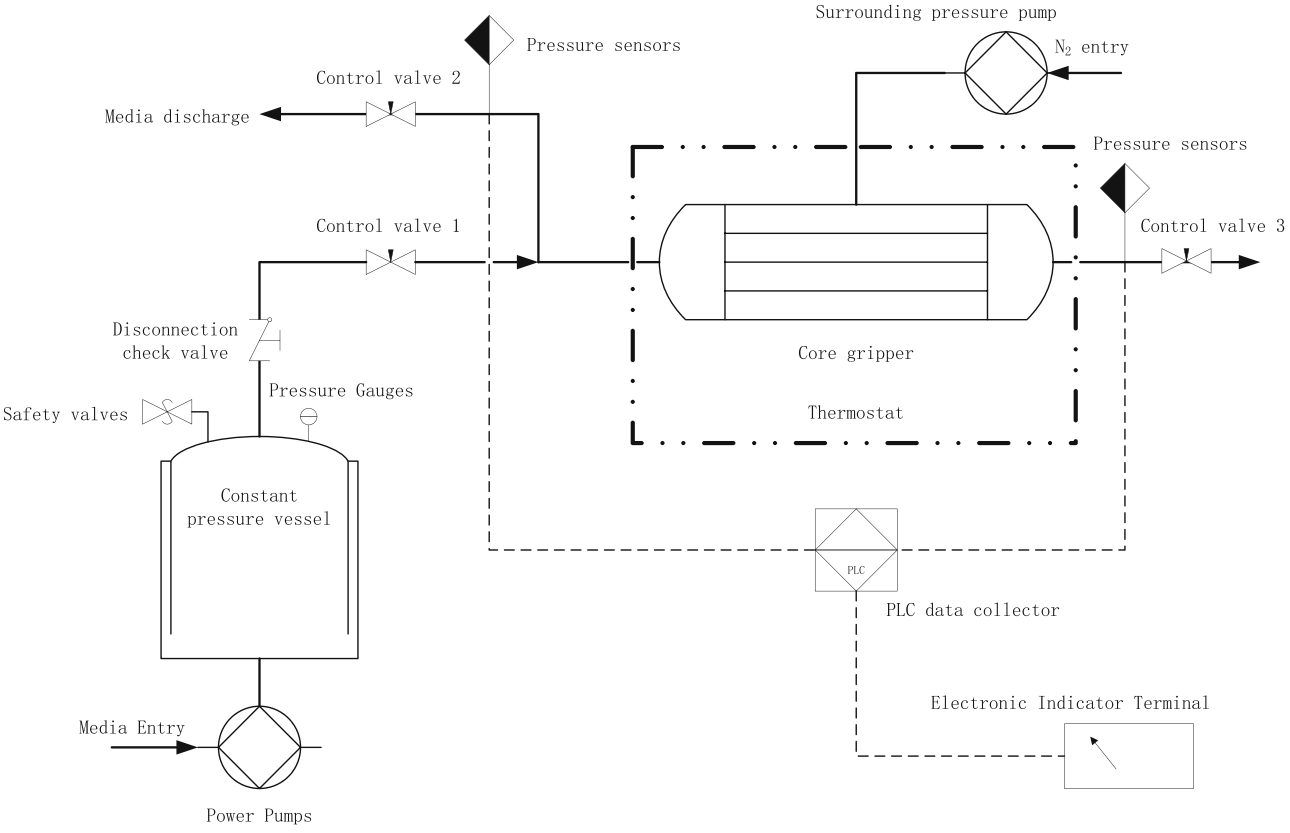

Figure 6: Diagram of dynamic imbibition measuring device.

standardize the data collected in order to effectively compare flowback behaviors and understand the underlying flowback mechanisms.

Sampling inspection is a statistical method used to assess the overall quality of a batch by inspecting a smaller number of representative samples. In this case, the data from 67 wells in the batch are being analyzed using Minitab software. The parameters used for the calculation include the batch size (67), acceptable quality level (AQL) (7.46%), rejected quality level (RQL) (17.91%), producer risk (alpha, 0.05), and consumer risk (beta, 0.10). To determine compliance with the description of fracturing fluid flowback characteristics, different sample sizes are considered. If the data from five representative wells in five secondary structural units are fully studied, it is judged that the description is basically compliant. On the other hand, if the data from 12 representative wells in a secondary structural unit are studied, it is determined that the description is fully compliant. The calculation follows the principle and formula of sampling inspection based on the principles of mathematical statistics. However, the specific calculation process and formula used in Minitab software are not provided in the given information. Calculate n (sample number) and c (acceptance number) as follows:

$$\alpha = 1 - \sum_{d=0}^{c} \frac{n!}{d!(n-d)!} p_1^d (1-p_1)^{n-d}, \tag{1}$$

$$\beta = \sum_{d=0}^{c} \frac{n!}{d!(n-d)!} p_2^d (1-p_2)^{n-d}, \tag{2}$$

where α is the producer risk, β is the consumer risk, p_1 is the AQL, and p_2 is the RQL or the percentage of defective products tolerated in batches.

Acceptance probability p_a describes the probability of accepting a specific batch based on a specific sampling plan and the ratio of defective products in the project, and the expression is as follows:

$$p_a = \sum_{d=0}^{c} \frac{n!}{d!(n-d)!} p^d (1-p)^{n-d}, \tag{3}$$

where c is the acceptance number, n is the number of samples, and p is the rate of defective products.

Rejection probability p_r describes the probability of rejecting a specific batch based on a specific sampling plan and the rate of incoming defective products, and the expression is as follows:

$$p_r = 1 - p_a, \tag{4}$$

where p_a is the acceptance probability.

The average detected quality AOQ represents the overall quality level of the project after inspection. The average detection quality varies with the rate of defective products, and the expression is as follows:

$$\mathrm{AOQ} = \frac{p_a p(N-n)}{N}, \tag{5}$$

where p_a is the acceptance probability, p is the defective product rate, N is the batch size, and n is the number of samples.

The average total inspection (ATI) number represents the average number of units to be inspected under a specific engineering quality level and acceptance probability; the expression is as follows:

$$\mathrm{ATI} = n + (1 - p_a)(N - n). \tag{6}$$

where p_a is the acceptance probability, N is the batch size, and n is the number of samples.

3.2 Experimental results

The determination of mineral composition of five core samples revealed that the average

TOC, brittle mineral content, and clay mineral content had little difference. However, the imbibition area differed significantly among the samples. These experimental results were obtained without considering the physical properties of shale.

The information that can be gathered from Figure 6 is as follows: (1) When exposed to the same experimental medium, the water absorption of different core samples is similar. However, core d in a distilled water medium exhibits a higher water absorption per unit area, measuring at 0.0165 g/cm^2, which is slightly higher than the other samples. (2) When considering the same core, the order of water absorption per unit area varies for different experimental media. The ranking of water absorption per unit area, from highest to lowest, is as follows: distilled water > formation water > fracturing fluid A > fracturing fluid B (Figure 7).

Based on Figures 8–12, the following information can be obtained: (1) The water absorption per unit area of all five core samples increases gradually over time, indicating a step-by-step upward trend. This behavior is consistent across all cores and experimental media. (2) Initially, core b exhibits a rapid increase in water absorption per unit area compared to the other cores under different experimental media conditions. The slope of its curve is much steeper. On the other hand, the curves of cores d and e appear relatively smooth, with a small comprehensive slope and a relatively small increase in water absorption per unit area. These curves also appear relatively flat.

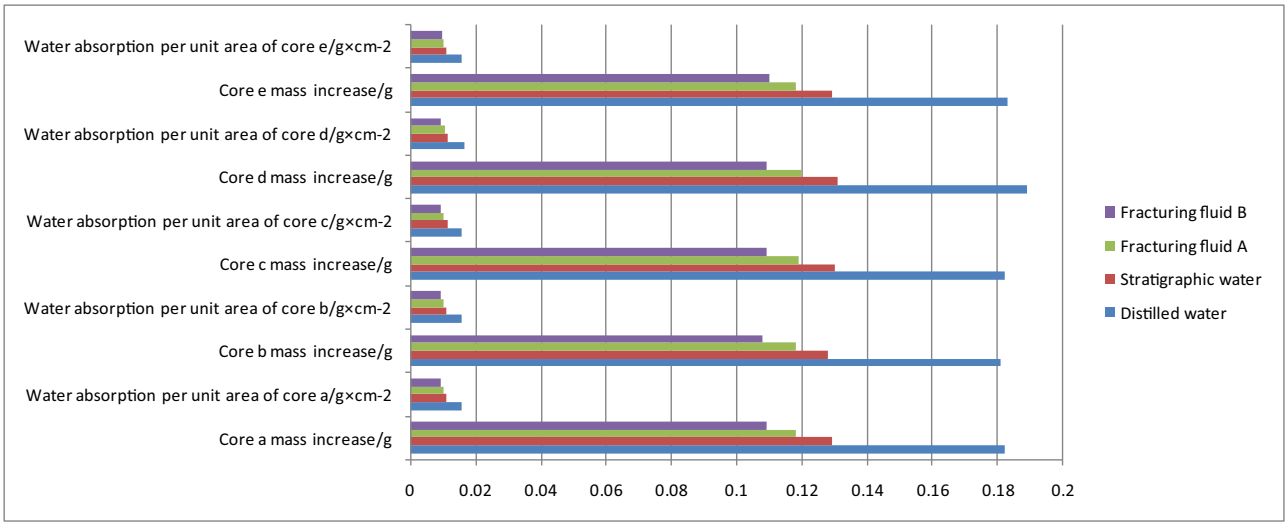

Figure 7: Results of static imbibition experiment.

(3) Core c takes longer to reach water absorption balance compared to the other cores, regardless of the experimental medium used. Specifically, the water absorption balance time for core c in distilled water is 25,000 min, indicating a delayed equilibrium state.

According to the research conducted by Villar, the temperature has a significant influence on the hydration expansion of clay minerals, especially when the temperature is higher than 100°C. However, this influence becomes weaker when the temperature is below 80°C. In the case of shale reservoirs, the compactness of the shale limits the effect of pressure on hydration expansion [26]. In the Jiangdong block, the shale reservoir has a maximum temperature of 80°C. Therefore, in the dynamic imbibition experiment, the temperature is set at 80°C, and the influence of pressure on shale hydration is disregarded. The experimental medium is only applied at a constant flow rate of 0.2 mL/min. After the dynamic experiment, it is observed that the experimental medium only infiltrates the shale cores superficially, and only cores d and e exhibit ductile intrusion along calcite vein fractures. This indicates that imbibition occurs primarily on the surface of compact shale after the liquid medium infiltrates the fractures. Hence, the imbibition area in the experiment is estimated as the sum of the core's end-face area and the area of fractured surfaces resulting from rubbing.

The information that can be gathered from Figure 13 is as follows: (1) When using the same experimental medium,

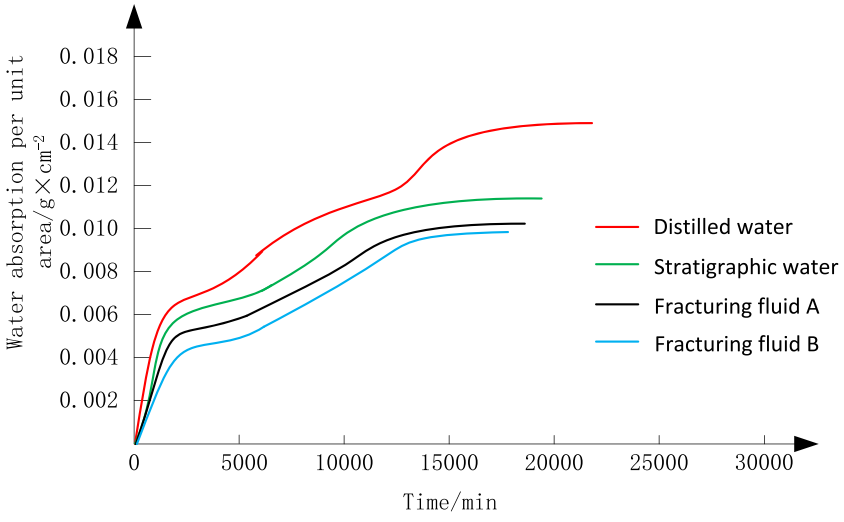

Figure 8: Relationship diagram of water absorption per unit area of core a with time change.

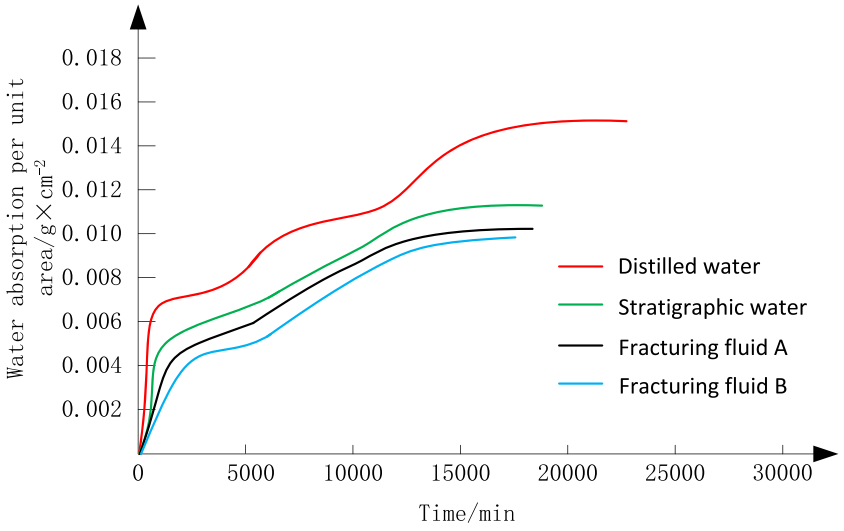

Figure 9: Relationship diagram of water absorption per unit area of core b with time change.

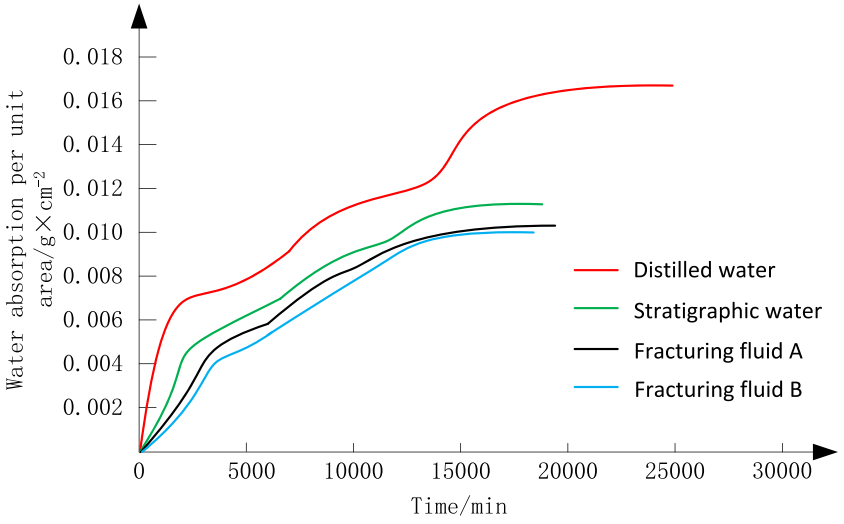

Figure 10: Relationship diagram of water absorption per unit area of core c with time change.

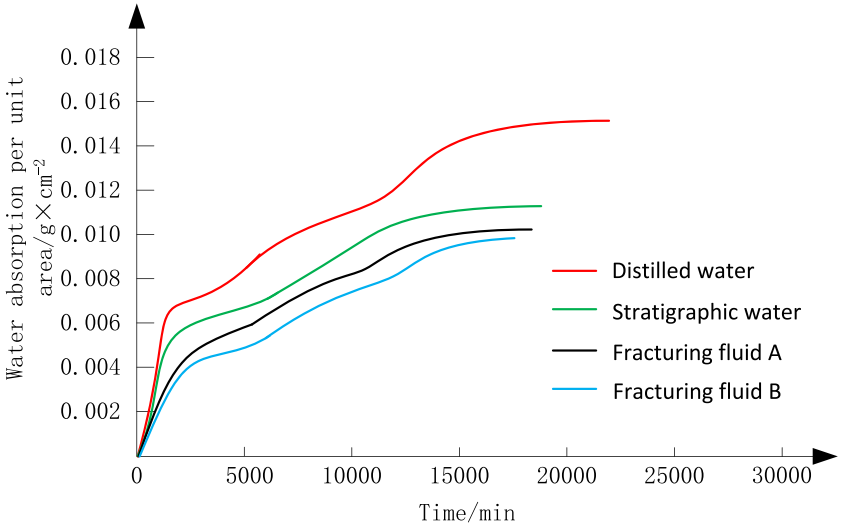

Figure 11: Relationship diagram of water absorption per unit area of core d with time change.

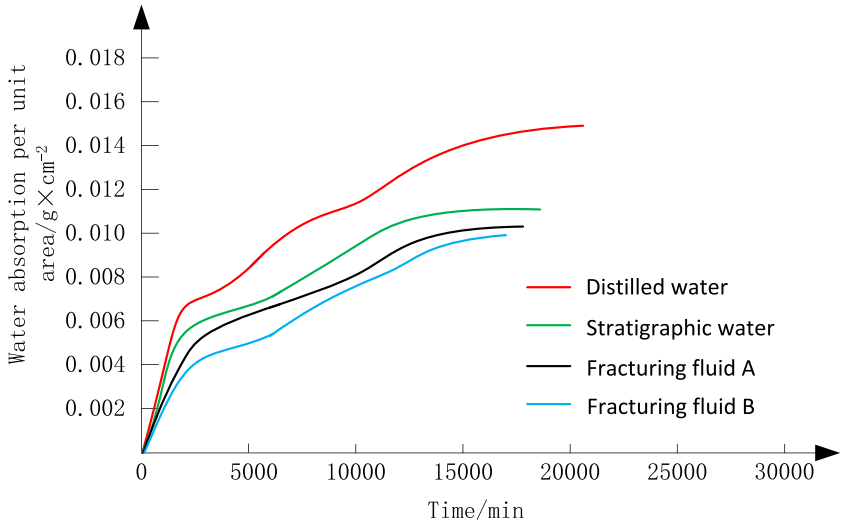

Figure 12: Relationship diagram of water absorption per unit area of core e with time change.

the order of water absorption by the cores is: d > e > c > b > a. (2) For each individual core, the order of experimental medium intake is as follows: distilled water > formation water > fracturing fluid A > fracturing fluid B. (3) Regardless of the type of experimental medium used, the imbibition area is directly proportional to the amount of water absorption. The highest water absorption value is 0.713 g when core d is displaced with distilled water, while the lowest value is 0.191 g when core b is displaced with fracturing fluid B. (4) Core d exhibits significantly higher overall water absorption compared to cores a and b. The water absorption of cores a and b is similar regardless of the medium used. Both fracturing fluids A and B have similar amounts of water absorption in all cores, with fracturing fluid A slightly higher in quantity compared to fracturing fluid B.

Through sampling inspection calculation, the result data in Table 2 and Figure 14 are obtained.

The information that can be gathered from Table 2 and Figure 14 is as follows: (1) When the actual defect reaches 7.46%, the probability of safe operation is 0.966, implying that there is a high likelihood of the system operating without any faults. The probability of further integrity evaluation is 0.034, indicating that there is a small chance that

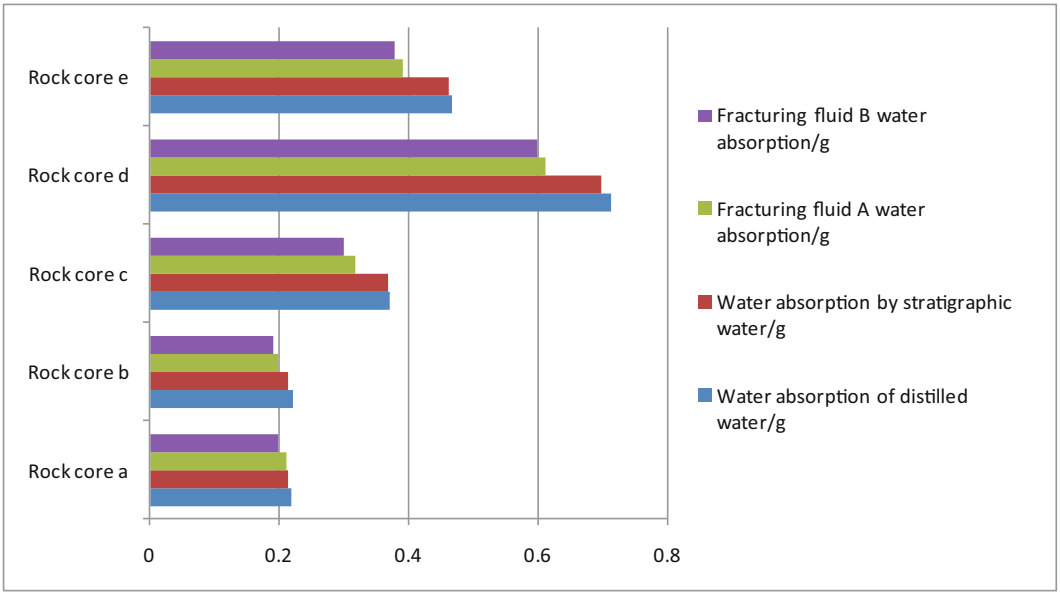

Figure 13: Results of dynamic imbibition experiment.

Table 2: Data of sampling inspection results

Defect (%)	Acceptance probability	Rejection probability	AOQ	ATI
7.46	0.966	0.034	5.380	18.7
35.82	0.091	0.909	2.432	62.5

additional assessments will be carried out. The average number of units inspected per batch is 18.7, meaning that a typical inspection will involve checking a total of 18.7 units. (2) When the actual defect reaches 35.82%, the probability of safe operation decreases significantly to 0.091, indicating a high risk of faults occurring. The probability of further integrity evaluation increases to 0.909, suggesting that additional assessments will likely be carried out. The average number of units inspected per batch increases to 62.5, showing that a larger sample size will be examined during the inspection. (3) Further calculations indicate that when the sample quality level is 16.689%, the average delivery quality limit will be 8.566%. This means that, on average, the quality of the delivered goods is limited to 8.566% defective units. (4) Based on the sampling scheme obtained, the data of all production from 17 wells controlled by any fault of 5 secondary structural units will be collected. Specifically, at least three wells under preset conditions will be selected for comparison. The preset conditions include a different shut-in time for the three wells, and similar fracturing fluids and fracturing scale will be used. Additionally, flowback data will be analyzed for the same shut-in time but under different secondary structural units. Data from 5 representative wells of 5 different secondary structural units out of the 17 will be screened for this comparative analysis.

4 Engineering verification

To compare the flowback data of two different fracturing fluids, A and B, the indoor experimental research results were expanded. The focus is on studying the flowback data under different secondary structural units and different shut-in times.

The sampling inspection scheme implemented involves collecting all production data from 17 wells under the control of any fault in 5 secondary structural units. The specific points of the scheme are as follows: (1) Table 3 presents the comparison of flowback data from three wells within the same secondary structural unit using fracturing fluid A but at different shut-in times. (2) Table 4 provides a comparative analysis of flowback data at the same shut-in time but under different secondary structural units using fracturing fluid B. The five wells screened for this analysis are coring wells with five cores used in the imbibition experiment. (3)

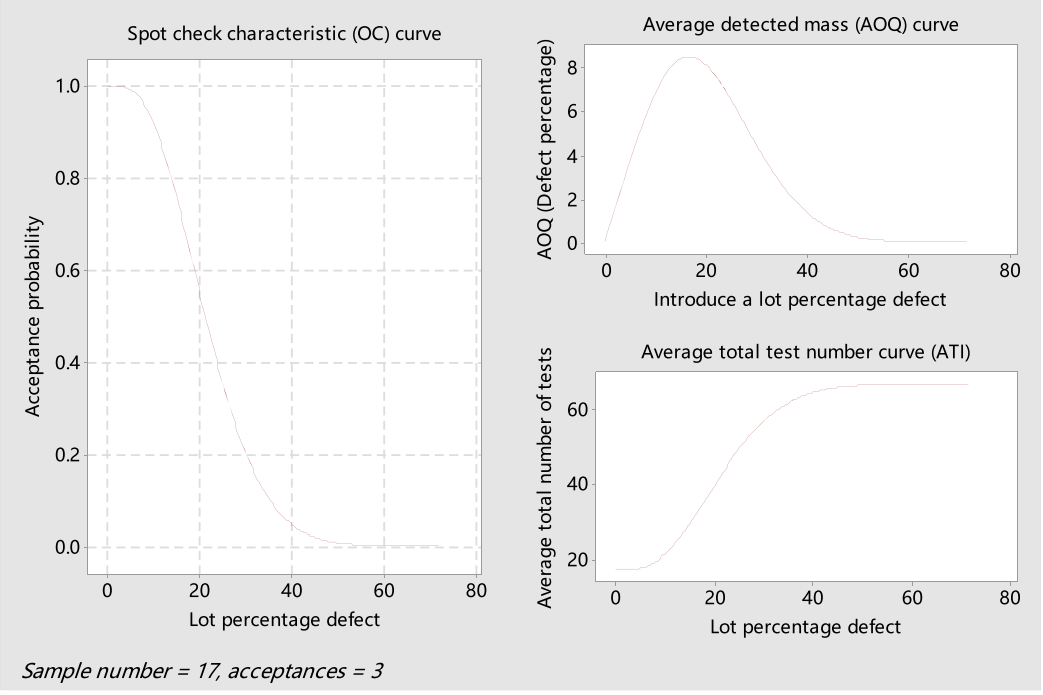

Figure 14: Sampling inspection result curve.

Table 3: Flowback data of same secondary structural unit at different shut-in times

Well	Shut-in time (days)	Total fracturing fluid volume (m^3)	Cumulative flowback (m^3)	Drain rate (m^3/days)	Reflux rate (%)	Test pressure (MPa)	Test output (m^3/days)
JY72-3	5	39926.92	11658.21	987.27	29.19	9.84	12.16×10^4
JY77-1	15	40952.99	9558.18	937.08	22.34	16.92	20.04×10^4
JY70-6	20	40753.75	8795.40	819.42	21.58	22.13	22.17×10^4

Fracturing fluid A demonstrates superior performance compared to fracturing fluid B. Fracturing fluid A uses a liquid as its basic agent and allows viscosity adjustment by adjusting the water content. On the other hand, fracturing fluid B uses a powdery solid as its basic agent and requires water to be added all at once to achieve the desired viscosity. (4) In terms of cost, fracturing fluid A is more beneficial compared to fracturing fluid B. Additionally, the storage and use of fracturing fluid A come with certain requirements, such as avoiding low temperatures during storage and observing a shelf life of 1 year. (5) It is important to note that JY70-6 and JY70-1 represent the same secondary structural unit and cluster well group. These wells share similar geological conditions, TOC levels, and physical parameters of the shale. This information provides an overview of the sampling inspection scheme and highlights the differences between fracturing fluids A and B in terms of performance and cost.

From Table 3, it can be observed that under the same secondary structural unit, a shorter shut-in time leads to a higher flowback rate and a lower test production. However, when the fracturing scale is similar, the difference in flowback rate among the three comparison wells is minimal. There is a slight gap in the test production, but this difference becomes smaller after a shut-in time of 15 days. It should be noted that the different drainage rates result in different test pressures, but these factors have been manipulated artificially and will not be discussed further.

From Table 4, under the premise of different secondary structural units, when the shut-in time is similar, the sequence of flowback rate is JY70-1 > JY74-5 > JY9 > JY81-2 > JY87-3, and the order of test output is JY70-1 > JY81-2 > JY74-5 > JY9 > JY87-3. It can be seen that there is a weak correlation between the flowback rate and the test yield. This phenomenon may be attributed to the different geological conditions, TOC levels, and physical properties of shale in different blocks.

Upon comparing the data of JY70-6 and JY70-1 wells constructed with fracturing fluid A and fracturing fluid B, respectively, several observations can be made. Under similar well conditions, the flowback rate of JY70-6 is slightly higher than that of JY70-1, while the production is slightly lower. This finding aligns with the conclusion drawn from the static imbibition experiment, which suggests that the unit area intake of fracturing fluid A is greater than that of fracturing fluid B. Furthermore, the dynamic imbibition experiment results indicate that the medium intake of fracturing fluid A is greater than that of fracturing fluid B in the core b experiment. However, despite these differences, the output of both wells does not exhibit a significant variance. Therefore, more parallel data are required to compare and optimize the effectiveness of the fracturing fluids.

To summarize, the practical observations obtained through the implementation of the sampling inspection scheme for engineering demonstration are consistent with the dynamic and static results obtained from the imbibition experiment. This study's conclusion can be considered valid and reliable.

Table 4: Typical well flowback data of five different secondary structural units

Core number	Well	Shut-in time (days)	Total fracturing fluid volume (m^3)	Cumulative flowback (m^3)	Drain rate (m^3/days)	Reflux rate (%)	Test pressure (MPa)	Test output (m^3/days)
d	JY87-3	17	38765.81	3557.87	323.44	9.18	15.23	8.22×10^4
b	JY70-1	20	41353.75	8574.4	779.49	20.73	28.21	23.78×10^4
c	JY9	19	39612.63	6321.33	574.67	15.96	16.58	9.35×10^4
e	JY81-2	20	38692.41	4215.83	383.26	10.90	19.46	20.24×10^4
a	JY74-5	18	40017.81	7842.27	722.78	19.59	20.68	19.11×10^4

5 Results and discussion

Based on the results of the imbibition experiment, the following information can be gleaned. The dynamic experiment demonstrates that the media intake varies depending on the viscosity, salinity, and water content of the experimental media used. In shale reservoirs, water absorption primarily occurs in the fracturing fluid. Therefore, in shale reservoirs with better fracturing effects and larger fracture network areas, the reservoir absorbs more water, making it more difficult to discharge the absorbed water. Consequently, the flowback rate is lower in these cases. Conversely, poor fracturing effects result in single fractures, with the fracturing fluid temporarily stored in large fractures and on the shale's surface. This leads to a higher flowback rate in engineering operations. Thus, under the same secondary structural unit, there exists an inverse relationship between the flowback rate and production output. The static experiments reveal that, for the same medium, the water absorption per unit area varies at different rates over time, due to differences in physical properties and the degree of microcracks. However, the overall trend remains the same. Among the cores tested, core b exhibits the fastest growth rate in water absorption per unit area over time. This suggests that to accurately calculate the water absorption of shale under formation conditions, it is necessary to obtain the corresponding salinity of formation water and conduct experiments accordingly. By knowing the area of the fracturing network, the water absorption of shale after fracturing can be inferred, laying the foundation for the calculation of the flowback rate.

The sampling inspection results provide the following information. In actual working conditions, due to variations in fracturing years and construction designs, the types of bridge plugs and fracturing fluids used are inconsistent, leading to irregular shut-in times for test wells. Therefore, it is not feasible to simply compare the data from the 67 wells that have been put into production in order to verify the accuracy of the imbibition test results. Instead, it is necessary to compare and analyze the flowback data under the same shut-in time but with different secondary structural units, as well as the flowback data under different shut-in times but with the same secondary structural unit. The specific scheme for this analysis is as follows: (1) Gather all production data from 17 wells that are under the control of any fault in 5 secondary structural units. Compare the data from at least three wells under preset conditions. (2) From the aforementioned 17 wells, select 5 representative wells from 5 different secondary structural units for continuous screening and comparative analysis. By following this scheme, a more accurate assessment of the imbibition test results can be obtained.

According to the engineering verification results, the following information can be obtained. By comparing the data in Table 3 with the results of the imbibition experiment, it can be concluded that a short shut-in time results in a short contact time between water in the fracturing fluid and the shale matrix. This leads to insufficient water absorption per unit area and an inadequate imbibition effect. After fracturing, a large amount of water enters the artificial fracture, which is then discharged, resulting in a high flowback rate. This finding is consistent with the results of the static imbibition experiment. By comparing the data in Table 4 with the results of the imbibition experiments, it can be concluded that the flowback rate at the same shut-in time, under the condition of different secondary structural units, follows the order JY70-1 > JY74-5 > JY9 > JY81-2 > JY87-3. The ranking order of representative cores conversion is b > a > c > e > d. This ranking is largely consistent with the results of the dynamic imbibition experiment, which measures the water absorption of cores. It can be inferred that a proper shut-in period after fracturing is beneficial for increasing production. This finding is consistent with the research results of Shel et al. [27], as the fracturing fluid's presence in the shale and its retention in fractures can provide support and improve productivity. These findings suggest that optimizing shut-in time is crucial for achieving optimal imbibition and production outcomes in shale reservoirs.

This study proposes the following scientific hypotheses: (1) Based on the imbibition experiment, the water absorption per unit area of the reservoir shale and the area of the fracturing network are known. With this information, the water absorption of the fractured reservoir can be calculated, allowing for the indirect prediction of the flowback rate. (2) The determination of the shut-in time can be guided by the dialysis equilibrium time of different shale reservoirs. In practical applications, the chloride ion content in the backflow fluid can be tested, and the stabilization time of the data can be used as a reference for determining the optimal shut-in time. These hypotheses provide valuable insights into understanding and optimizing the production behavior of shale reservoirs. Further research and experimentation can be conducted to validate and expand upon these hypotheses.

The primary objective of this study is to investigate the relationship between the flowback rate, shut-in time, and production of shale gas wells following fracturing. This will be achieved through a combined analysis of experimental data and engineering insights. In comparison to prior research, there are notable distinctions: (1) Our research integrates both method-oriented and result-oriented approaches. Building on traditional imbibition experiments, we distinguish between

dynamic and static situations. Moreover, we address the challenges associated with messy, irregular, and statistically unanalyzable original production test well data. In contrast, earlier studies primarily focused on optimizing the imbibition process, expanding its functionality, and enhancing result accuracy, without adequately addressing the engineering problems at hand (such as those discussed by Cai [28] and Liu et al. [29]). (2) Our research involves imbibition experiments conducted on four media, employing five core samples. We extensively examine the relationship between water absorption per unit area and time for various cores immersed in different media. The experiment is designed with an optimal configuration and a simple process, making it easily adaptable to production sites and reproducible by other researchers. Conversely, many other experiments rely heavily on costly and complex equipment, such as scanning electron microscopes, nuclear magnetic resonance core analysis instruments, and fluid scanning imaging tools. These excessive resources are often unnecessary for addressing engineering problems, and many developing countries and production sites lack the necessary means to carry out such research (as highlighted in previous studies [30–32]).

Although our research aims to closely simulate the conditions at the production site and proposes a comprehensive experimental workflow combining inspection, there are certain limitations in data rigor and method perfection that need to be acknowledged. These include the following: (1) The influence of fractures in shale reservoirs on adsorption and flowback was not taken into account in our study. This is because accurately determining the degree and volume of cracks in a laboratory environment is challenging. As a result, there might be some errors in determining the imbibition area in this study. (2) In the dynamic imbibition experiment, all cores were dried in an oven at a temperature of 110°C for 24 h. However, this step raises the question of whether it ignores the influence of the initial water saturation of the original shale reservoir on the experimental results. (3) Previous studies have shown that water absorption in shale is comprised of surface hydration water absorption, osmotic hydration water absorption, and capillary water absorption [33]. In this study, the experimental data under the condition of formation water medium are not fully utilized, and the influence of high mineral pore water on shale osmotic hydration is not discussed. Therefore, the rigor of the study regarding the hydration ability of the shale reservoir is not fully addressed. (4) Due to limitations in the available data from overall sample wells in the study area and a dearth of parallel data from comparison wells, the conclusions drawn from this single experiment and its engineering validation may not be sufficient for confidently judging the quality of fracturing fluid.

The novelty of this study can be summarized as follows: (1) This study addresses engineering problems by proposing a workflow for analyzing fracturing fluid flowback in specific blocks. This workflow is based on core experiments and engineering demonstrations, providing a practical approach for solving these problems. (2) The main steps of the proposed workflow are “imbibition experiment → sampling inspection → engineering verification.” This workflow is highly practical, with a short and effective process. It is not limited by the availability of single well data, and the results can be reasonably and cost-effectively verified using messy engineering data. (3) The study focuses on the Jiangdong block of Fuling shale gas, and contributes to the establishment of an experimental scheme for imbibition inclusion. The results obtained from this study can serve as valuable guidance for future engineering projects in this block.

6 Conclusion

The focus of this study is on the Jiangdong block of Fuling shale gas, where the research aims to investigate the mechanism of fracturing fluid flowback during production testing. Core imbibition experiments and sampling inspections are utilized as verification methods in the production test. The engineering significance of this study stems from several challenges. First, the data obtained from conventional production test wells in this block are disorganized, irregular, and not suitable for statistical analysis. Additionally, the production line lacks theoretical support, and there is a lack of experimental results regarding imbibition in production wells. To address these challenges, this study combines the typical core test results from 5 secondary structural units with data from 67 completed and production-tested wells. Sampling inspections are carried out with cost considerations in mind. By doing so, the study systematically examines the characteristics of flowback data with the same shut-in time under different secondary structural units, as well as different shut-in times under the same secondary structural unit. This research contributes to the field by providing a comprehensive understanding of the flowback process in the Jiangdong block of Fuling shale gas. The adoption of core imbibition experiments and sampling inspections, along with the integration of various datasets, improves the statistical analysis capabilities and theoretical foundation of the production line.

There exists a relationship between flowback rate, shut-in time, and production following fracturing in shale gas wells. The imbibition experiment demonstrates that imbibition occurs solely on the surface of tight shale after

the intrusion of the liquid medium into the fracture, with the extent of water absorption being directly proportional to the imbibition area. The engineering verification results, obtained from the sampling inspection scheme, reveal that a shorter shut-in time corresponds to higher flowback rates and lower test production within the same secondary structural unit. When the shut-in time is similar across different secondary structural units, the correlation between flowback rate and test production is weak. In terms of engineering expansion, shale hydration leads to the absorption of water from the fracturing fluid. Consequently, when selecting and formulating fracturing fluids, the objective should be to minimize shale hydration and enhance the sand-carrying effect. By reducing the amount of water absorbed by the shale during the fracturing process, the return rate of the fracturing fluid can be improved, thereby reducing reservoir damage and increasing production. In the next phase, core samples exhibiting significant differences in physical properties should be chosen, and experiments should be conducted to evaluate the impact of mineral composition and pore size on permeability and adsorption before and after core seepage.

Acknowledgements: The authors thank the following organizations for funding and supporting this project: National Natural Science Foundation of China (41572322), Heilongjiang Provincial Natural Science Foundation of China (LH2020E089), The Natural Science Foundation of the Jiangsu Higher Education Institutions of China (23KJA460004), Basic Scientific Research Program of Nantong City (JC22022014), Outstanding Young Core Teachers from "Green-Blue Project" of Colleges and Universities in Jiangsu Province, Young and Middle-aged Academic Leaders from "Green-Blue Project" of Colleges and Universities in Jiangsu Province, Scientific Research Start-up Fund for Talent Introduction at Jiangsu College of Engineering and Technology, and China Petrochemical Shale Gas "Ten Dragons" Science and Technology Research Project (P18051).

Author contributions: Ye Yang: conceptualization, methodology, writing – original draft, and writing – review and editing; Yawovi Souley Agbodjan: conceptualization, methodology, writing – original draft, and writing – review and editing. Bo Liang: conceptualization, methodology, writing – original draft, and writing – review and editing.

Conflict of interest: The authors declare that they have no known competing financial interests or personal relationships that could have appeared to influence the work reported in this article.

Data availability statement: The data that support the findings of this study are available in this article.

References

[1] Sun Z. Superimposed hydrocarbon accumulation through multi-source and multi-stage evolution in the Cambrian Xixiangchi Group of eastern Sichuan Basin: a case study of the Pingqiao gas-bearing anticline. Energy Geosci. 2023;4(1):131–42.
[2] Wu Z, Cui C, Jia P, Wang Z, Sui Y. Advances and challenges in hydraulic fracturing of tight reservoirs: A critical review. Energy Geosci. 2022;3(4):427–35.
[3] Zhu QY, Dai J, Yun FF, Zhai HH, Zhang M, Feng LR. Dynamic response and fracture characteristics of granite under microwave irradiation. J Min Strata Control Eng. 2022;4(1):019921.
[4] Qu Z, Wang J, Guo T, Shen L, Liao H, Liu X, et al. Optimization on fracturing fluid flowback model after hydraulic fracturing in oil well. J Pet Sci Eng. 2021;204:108703.
[5] Chen Q, Wang F. Mathematical modeling and numerical simulation of water–rock interaction in shale under fracturin-fluid flowback conditions. Water Resour Res. 2021;57(8):e2020WR029537.
[6] Liu J, Xue Y, Liang X, Wang S. Numerical simulation of proppant migration in fractal fractures during fracturing fluid flowback. Arab J Sci Eng. 2023;48(7):9369–81.
[7] Wang S, Bai Y, Xu B, Li Y, Chen L, Dong Z, et al. A hybrid model for simulating fracturing fluid flowback in tight sandstone gas wells considering a three-dimensional discrete fracture. Lithosphere. 2021;2021(Special 4):7673447.
[8] Elputranto R, Cirdi AP, Akkutlu IY. Formation damage mechanisms due to hydraulic fracturing of shale gas wells. SPE Europec. OnePetro; 2020.
[9] Hun L, Bing Y, Xixiang S, Xinyi S, Lifei D. Fracturing fluid retention in shale gas reservoir from the perspective of pore size based on nuclear magnetic resonance. J Hydrol. 2021;601:126590.
[10] Al Shidhani R, Al Shueili A, Al Salmi H, Jaboob M. Impact of delayed flowback on well performance: case study. SPE International Hydraulic Fracturing Technology Conference & Exhibition. SPE, 2022. p. D011S004R004.
[11] Saini RK, Crane B, Shimek NR, Wang W, Cooper B. Enhanced regained permeability and fluid flowback from tight sandstone and carbonate oil reservoirs with unique flowback chemistry. Can J Chem Eng. 2022;100(6):1309–22.
[12] Osselin F, Nightingale M, Hearn G, Kloppmann W, Gaucher E, Clarkson CR, et al. Quantifying the extent of flowback of hydraulic fracturing fluids using chemical and isotopic tracer approaches. Appl Geochem. 2018;93:20–9.
[13] Owen J, Bustin RM, Bustin AMM. Insights from mixing calculations and geochemical modeling of Montney Formation post hydraulic fracturing flowback water chemistry. J Pet Sci Eng. 2020;195:107589.
[14] Wu YN, Tang LS, Li Y, Zhang LY, Jin X, Zhao MW, et al. Probing the influence of secondary fracture connectivity on fracturing fluid flowback efficiency. Pet Sci. 2023;20(2):973–81.
[15] Yang F, Zheng H, Guo Q, Lyu B, Nie S, Wang H. Modeling water imbibition and penetration in shales: New Insights into the retention of fracturing fluids. Energy Fuels. 2021;35(17):13776–87.

[16] Verdugo M, Doster F. Impact of capillary pressure and flowback design on the clean up and productivity of hydraulically fractured tight gas wells. J Pet Sci Eng. 2022;208:109465.
[17] Wang B, Liu B, Yang J, Bai L, Li S. Compatibility characteristics of fracturing fluid and shale oil reservoir: A case study of the first member of Qingshankou Formation, northern Songliao Basin, Northeast China. J Pet Sci Eng. 2022;211:110161.
[18] Chen F, Wang K, Luo M, Bu T, Yuan X, Du G, et al. Treatment and recycling of acidic fracturing flowback fluid. Environ Technol. 2022;43(15):2310–8.
[19] Shaibu R, Guo B. The dilemma of soaking a hydraulically fractured horizontal shale well prior to flowback–A decade literature review. J Nat Gas Sci Eng. 2021;94:104084.
[20] Nguyen-Le V, Shin H. Development of reservoir economic indicator for Barnett Shale gas potential evaluation based on the reservoir and hydraulic fracturing parameters. J Nat Gas Sci Eng. 2019;66:159–67.
[21] Suboyin A, Rahman MM, Haroun M. Hydraulic fracturing design considerations, water management challenges and insights for Middle Eastern shale gas reservoirs. Energy Rep. 2020;6:745–60.
[22] Jia A, Hu D, He S, Guo X, Hou Y, Wang T, et al. Variations of pore structure in organic-rich shales with different lithofacies from the Jiangdong block, fuling shale gas field, SW China: Insights into gas storage and pore evolution. Energy Fuels. 2020;34(10):12457–75.
[23] Nie H, Li P, Dang W, Ding J, Sun C, Liu M, et al. Enrichment characteristics and exploration directions of deep shale gas of Ordovician–Silurian in the Sichuan Basin and its surrounding areas, China. Pet Explor Dev. 2022;49(4):744–57.
[24] Nie H, Li D, Liu G, Lu Z, Hu W, Wang R, et al. An overview of the geology and production of the Fuling shale gas field, Sichuan Basin, China. Energy Geosci. 2020;1(3–4):147–64.
[25] Trouvé R, Arthur AD, Robinson AP. Assessing the quality of offshore Binomial sampling biosecurity inspections using onshore inspections. Ecol Appl. 2022;32(5):e2595.
[26] Villar MV, Lloret AJ. Influence of temperature on the hydro-mechanical behaviour of a compacted bentonite. Appl Clay Sci. 2004;26(1–4):337–50.
[27] Shel E, Paderin G, Kazakov E, Sayfutdinov E, Gaynetdinov R, Uchuev R, et al. Technological and economical optimization of a hydraulic fracturing design: choice of proppant, liquid and pump schedule. SPE Symposium: Hydraulic Fracturing in Russia. Experience and Prospects. OnePetro; 2020.
[28] Cai MF. Key theories and technologies for surrounding rock stability and ground control in deep mining. J Min Strata Control Eng. 2020;2(3):5–13.
[29] Liu J, Sheng JJ, Huang W. Experimental investigation of microscopic mechanisms of surfactant-enhanced spontaneous imbibition in shale cores. Energy Fuels. 2019;33(8):7188–99.
[30] Wang X, Wang M, Li Y, Zhang J, Li M, Li Z, et al. Shale pore connectivity and influencing factors based on spontaneous imbibition combined with a nuclear magnetic resonance experiment. Mar Pet Geol. 2021;132:105239.
[31] Li J, Li H, Yang C, Ren X, Li Y. Geological characteristics of deep shale gas and their effects on shale fracability in the Wufeng-Longmaxi formations of the Southern Sichuan Basin, China. Lithosphere. 2023;2023(1):4936993.
[32] Kibria MG, Hu Q, Liu H, Zhang Y, Kang J. Pore structure, wettability, and spontaneous imbibition of Woodford shale, Permian Basin, West Texas. Mar Pet Geol. 2018;91:735–48.
[33] Roshan, H, Andersen MS, Rutlidge H, Marjo CE, Acworth RI. Investigation of the kinetics of water uptake into partially saturated shales. Water Resour Res. 2016;52:2420–38.